

Chaotic duality in string theory

Sebastián Franco,^{1,*} Yang-Hui He,^{2,†} Christopher Herzog,^{3,‡} and Johannes Walcher^{3,§}

¹*Center for Theoretical Physics, Massachusetts Institute of Technology, Cambridge, Massachusetts 02139, USA*

²*Department of Physics and Math/Physics RG, The University of Pennsylvania, Philadelphia, Pennsylvania 19104, USA*

³*Kavli Institute for Theoretical Physics, University of California, Santa Barbara, California 93106, USA*

(Received 29 April 2004; published 27 August 2004)

We investigate the general features of renormalization group flows near superconformal fixed points of four dimensional $\mathcal{N}=1$ gauge theories with gravity duals. The gauge theories we study arise as the world-volume theory on a set of D-branes at a Calabi-Yau singularity where a del Pezzo surface shrinks to zero size. Based mainly on field theory analysis, we find evidence that such flows are often chaotic and contain exotic features such as duality walls. For a gauge theory where the del Pezzo is the Hirzebruch zero surface, the dependence of the duality wall height on the couplings at some point in the cascade has a self-similar fractal structure. For a gauge theory dual to P^2 blown up at a point, we find periodic and quasiperiodic behavior for the gauge theory couplings that does not violate the a conjecture. Finally, we construct supergravity duals for these del Pezzos that match our field theory beta functions.

DOI: 10.1103/PhysRevD.70.046006

PACS number(s): 11.25.Mj, 11.10.Gh, 11.15.Pg

I. INTRODUCTION AND SUMMARY

Understanding renormalization group flows out of conformal fixed points of supersymmetric gauge theories is of vital importance in fully grasping the AdS-CFT correspondence beyond superconformal theories and brings us closer to realistic gauge theories such as QCD. In particular, the $\mathcal{N}=1$ gauge theories arising from world-volume theories of D-brane probes on Calabi-Yau singularities have been extensively studied under this light. Dual to these theories are the so-called nonspherical horizons of AdS [1,2].

A prominent example, the conifold singularity, was analyzed by Klebanov and Strassler (KS) in [3] where the RG flow takes the form of a duality cascade. Here, we have a theory with two gauge group factors and four associated bi-fundamental fields. With the addition of appropriate D5-branes, the theory is taken out of conformality in the infrared. Subsequently, the two gauge couplings evolve according to non-trivial beta functions. Whenever one of the couplings becomes strong, we should perform Seiberg duality to migrate into a regime of weak coupling [3]. And so on do we proceed *ad infinitum*, generating an intertwining evolution for the couplings. This is called the KS cascade. The dual supergravity (SuGRA) solution, happily aided by our full cognizance of the metric on the conifold, can be studied in detail and matches the field-theory behavior.

One would imagine that a similar analysis, applied to more general Calabi-Yau singularities than the conifold, could be performed, *mutatis mutandis*. Indeed, a full field theory treatment can be undertaken using various techniques for constructing the gauge theory for D-brane probes on wide classes of singularities. Behavior that differs dramatically from the KS flow has been subsequently observed for, *exem-*

pli gratia, a class of nonspherical horizons which are $U(1)$ bundles over the del Pezzo surfaces [4,5]. Using the a -maximization procedures of [6,7] to determine anomalous dimensions and beta functions, the numerical studies of [5] have convinced us that, sensitive to the type of geometry as well as initial conditions, the quivers after a large number of Seiberg dualities may become hyperbolic in the language of [8]. After this, a finite energy scale is reached beyond which duality cannot proceed. This phenomenon has been dubbed a “duality wall” by [9].

The purpose of this paper was to elucidate some aspects of flows, cascades, and walls for gauge theories arising from these more general geometries using both field theory and SuGRA techniques. To begin with, a more systematic, and where possible, analytic investigation of the duality wall phenomenon is clearly beckoning. For this purpose, we will use the exceptional collection techniques that become particularly conducive for the del Pezzo surfaces [10], especially for computing the beta functions and Seiberg dualities [11,12]. We review these matters synoptically in Sec. II. In particular, we will formulate the general RG cascade as motion and reflections in certain *simplices* in the space of gauge couplings.

Thus girt with the analytic form of the beta functions and Seiberg duality rules [5,11,12], we show in Sec. III the existence of the duality wall at finite energy. As an illustrative example, we focus on F_0 , the zeroth Hirzebruch surface. In the numerical studies of [5], two types of cascading behavior were noted for F_0 . Depending on initial values of couplings, one type of cascade readily caused the quiver to become hyperbolic and hence an exponential growth of the ranks, whereby giving rise to a wall. The other type, though seemingly asymptoting to a wall, was not conclusive from the data. As an application of our analytic methods, we show that duality walls indeed exist for both types and give the position thereof as a function of the initial couplings. These results represent the first example in which the position of a duality wall along with all the dual quivers in the cascade have been analytically determined. Thus, we consider it to be

*Email address: sfranco@mit.edu

†Email address: yanghe@physics.upenn.edu

‡Email address: herzog@kitp.ucsb.edu

§Email address: walcher@kitp.ucsb.edu

an interesting candidate to attempt the construction of a SuGRA dual. Interestingly, the duality wall height function is piece-wise linear [4,5] and “fractal.” A highlight of this section will be the demonstration that a *fractal* behavior is indeed exhibited in such RG cascades. As we zoom in on the wall-position curve, a self-similar pattern of concave and convex cusps emerges.

Inspired by this *chaotic behavior*, we seek further in our plethora of geometries for signatures of chaos. Moving onto the next simplest horizon, namely that of the dP_1 , the first del Pezzo surface, we again study the analytic evolution of the cascade in detail. Here, we find Poincaré cycles for trajectories of gauge coupling pairs. The shapes of these cycles depend on the initial values of couplings. For some ranges, beautiful elliptical orbits emerge. This type of behavior is reminiscent of the attractors and Russian doll renormalization group flow discussed in [13]. This example constitutes Sec. IV.

Finally, in Sec. V, we move on to the other side of the AdS-CFT correspondence and attempt to find SuGRA solutions. We rely upon the methodologies of [14] to construct solutions that are analogous to those of Klebanov and Tseytlin (KT) [15] for the conifold. The fact that explicit metrics for cones over del Pezzo surfaces are not yet known is only a minor obstacle. We are able to write down KT-like solutions, complete with the warp factor, as an explicit function of the Cartan matrices of the exceptional algebra associated with the del Pezzo.

These SuGRA solutions should be dual to field theory cascades that are similar to the original KS cascade. Identifying the precise SuGRA phenomenon which marks the duality wall remains an open and tantalizing quest.

We would like to stress the importance of possible corrections to the R-charges of the matter fields, and hence to the anomalous dimensions and beta functions. We will see that in order to be able to follow the RG cascades accurately, we need to be able to assume that the R-charges are corrected only at order $\mathcal{O}(M/N)^2$ where M is the number of D5-branes, N the number of D3-branes, and M/N a measure of how close we are to the conformal point $M=0$. In the case of the conifold, the gauge theory possessed a \mathbb{Z}_2 symmetry which forced the $\mathcal{O}(M/N)$ corrections to vanish. Our del Pezzo gauge theories generally lack such a symmetry.

We have two arguments to address these concerns. First, for KS type cascades, our SuGRA solutions match the field theory beta functions precisely, severely constraining any possible M/N corrections to the R-charges. For more complicated cascades involving duality walls, we lack SuGRA solutions. Nevertheless, we shall push ahead, assuming that eventually appropriate supergravity solutions will be found and that R-charge corrections, even if $\mathcal{O}(M/N)$, will not change the qualitative nature of our results. The flows which we shall soon present are so interesting that we think it worthwhile to describe them in their current, though less than fully understood state. An analogy can be made to the Navier-Stokes equation. Turbulence is observed in fluids in many different situations but is very difficult to model exactly. Instead, people have developed simple models, such as Feigenbaum’s quadratic recursion relation, to understand cer-

tain qualitative features, such as period doubling. In some sense, the flows we present here are in relation to the real RG flows as Feigenbaum’s analysis is to the real Navier-Stokes equation.

II. A SIMPLICIAL VIEW OF RG FLOW

In preparation for our discussions on renormalization group (RG) flow in the gauge theory duals to del Pezzo horizons, we initiate our study with an abstract and recollective discussion of RG flows and duality cascades.

A. The Klebanov-Strassler cascade

The Klebanov-Strassler (KS) flow [3] provides our paradigm for an RG cascade. In the KS flow, one starts with an $\mathcal{N}=1$ $SU(N) \times SU(N+M)$ gauge theory with bifundamental chiral superfields A_i and B_i , $i=1,2$ and a quartic superpotential. The couplings associated with the two gauge groups we shall respectively call g_1 and g_2 . This quiver theory can be geometrically realized as the world-volume theory of a stack of N coincident D3-branes together with M D5-branes probing a conifold singularity. The matter content and superpotential are given as follows:

$$\begin{array}{c} \text{A}_{1,2} \\ \bullet \xleftarrow{\quad} \bullet \xrightarrow{\quad} \\ \text{B}_{1,2} \end{array} \quad \begin{array}{c} N \\ N+M \end{array} \quad W = \frac{\lambda}{2} \epsilon^{ij} \epsilon^{kl} \text{Tr } A_i B_k A_j B_l \quad (2.1)$$

where λ is the superpotential coupling and the trace is taken over color indices.

For $M=0$ the gauge theory is conformal. Indeed, the M D5-branes are added precisely to take us out of this conformal point, inducing a RG flow.

The one loop NSVZ beta function [16] determines the running of the gauge couplings. For each gauge group we have

$$\beta_i = \frac{d(8\pi^2/g_i^2)}{d \ln \mu} = \frac{3T(G) - \sum_i T(r_i)(1-2\gamma_i)}{1 - \frac{g_i^2}{8\pi^2} T(G)} \quad (2.2)$$

where μ is a ratio of energy scales and for an $SU(N_c)$ gauge group $T(G)=N_c$ and $T(fund)=1/2$.

Using $\gamma_i = \frac{3}{2}R_i - 1$, we can express the beta functions $\beta_{i=1,2}$ for the two gauge couplings $g_{i=1,2}$ in terms of R-charges. As is done in [3], we will work in the approximation that the denominator of Eq. (2.2) is neglected. Then, the beta functions become

$$\beta_1 = 3[N + (R_A - 1)(N + M) + (R_B - 1)(N + M)],$$

$$\beta_2 = 3[(N + M) + (R_A - 1)N + (R_B - 1)N].$$

At the conformal point, the R-charges of the bifundamentals can be calculated from the geometry and are $R_A = R_B = 1/2$. They can also be simply determined by using the

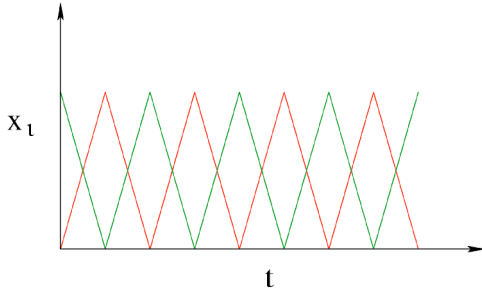


FIG. 1. The KS cascade for the conifold. The two inverse gauge couplings $x_{i=1,2} = 1/g_i^2$ for the two nodes evolve in weave pattern against log-energy scale t where Seiberg duality is applied whenever one of the x_i 's reaches zero.

symmetries of the quiver and requesting the vanishing of the beta functions for the gauge and superpotential couplings. Generically, we would expect the R-charges to suffer $\mathcal{O}(M/N)$ corrections for $M \neq 0$. Here however, there is a \mathbb{Z}_2 symmetry $M \rightarrow -M$ for large N that forces the corrections to be of order at least $\mathcal{O}(M/N)^2$. Thus,

$$\beta_1 = -3M, \quad \beta_2 = 3M \quad (2.3)$$

up to $\mathcal{O}(M/N)$ corrections.

If we trust these one loop beta functions, then flowing into the IR, we see that the coupling g_2 will eventually diverge because of the positivity of β_2 . According to Klebanov and Strassler, the appropriate remedy is a Seiberg duality. After the duality, the gauge group becomes $SU(N) \times SU(N-M)$ but otherwise the theory remains the same. After this duality, the beta functions change sign $\beta_1 = 3M$ and $\beta_2 = -3M$. This process of Seiberg dualizing and flowing can be continued for a long time in the large N limit as shown in Fig. 1. The number of colors in the gauge groups becomes smaller and smaller. Klebanov and Strassler [3] demonstrated that when one of the gauge groups becomes trivial, the gauge theory undergoes chiral symmetry breaking and confinement. The phenomenon is realized geometrically in the SuGRA dual by a deformation of the conifold in the IR.

Clearly there are some weaknesses in this purely gauge theoretic approach to the RG flow of a strongly coupled gauge theory. Usually Seiberg duality is understood as an IR equivalence of two gauge theories and is not performed in the limit $g_2 \rightarrow \infty$. Can we really trust Seiberg duality here? Also, we have dropped the denominator of the full NSVZ beta function (2.2), which is presumably important. Nevertheless, the analysis is sound and the strongest argument for the validity of these Seiberg dualities comes not from gauge theory but from the dual supergravity theory [3]. There is a completely well-behaved supergravity solution, the KS solution of the conifold, which models this RG flow. On the gravity side, there is a radial dependence of the 5-form flux which produces a logarithmic running of the effective number of D3-branes in complete accordance with the field theory cascade, giving credence to these Seiberg dualities.

B. General RG flows

We shall henceforth focus on the four dimensional, $\mathcal{N} = 1$ gauge theories engineered by placing D3-branes at the singularity of a Calabi-Yau threefold cone over a del Pezzo surface (cf. e.g. [11,17–20] for a comprehensive discussion). With some important caveats, these theories can be treated in a fashion similar to the discussion above for the conifold.

The field content of a del Pezzo gauge theory is described compactly by a quiver. For D-branes probing the n -th del Pezzo, the number of gauge group factors in the quiver theory is equal to

$$k = n + 3, \quad (2.4)$$

which is the Euler characteristic $\chi(dP_n)$. We reserve the index $i = 1, 2, \dots, k$ for labeling the nodes of the quiver. We denote the adjacency matrix of the quiver by f_{ij} . In other words, f_{ij} is the number of arrows in the quiver from node i to node j . We point out that by definition, the f_{ij} are all non-negative.

Thus given a quiver, we need to specify the ranks of the gauge groups in order to define a gauge theory. We will denote the rank of the gauge group on the i -th node by d^i , and the dimension vector by $d = (d^i)_{i=1, \dots, k}$. As on the conifold, the ranks d^i are related to the number of branes that realize the specific gauge theory in string theory. When probing the del Pezzos, we will reserve N to denote the number of regular D3-branes, and M^I to denote the number of D5-branes. The D3-brane corresponds to a unique dimension vector which we will denote by $r = (r^i)_{i=1, \dots, k}$. In distinction to the conifold and its ADE generalizations, the possible D5-branes are constrained by chiral anomaly cancellation, and we will parametrize their dimension vectors by $s_I = (s_I^i)_{i=1, \dots, k}$ with $I = 1, 2, \dots, n$.

Summarizing, a D-brane configuration with N regular D3-branes and M^I D5-branes of type I corresponds to the gauge group $\prod_{i=1}^k SU(d^i)$ with

$$d^i = r^i N + s_I^i M^I \quad (2.5)$$

and f_{ij} chiral fields X_{ij} in the $SU(d^i) \times SU(\overline{d^j})$ bifundamental representation.

As shown in [11,12], the beta functions of the gauge theory can be computed effectively from geometry by taking advantage of the exceptional collection language [10–12,21]. An exceptional collection $\mathcal{E} = (E_1, E_2, \dots, E_k)$ is an ordered collection of sheaves, specifying the D-brane associated with each node. The intersections of the sheaves give rise to massless strings which in turn correspond to bifundamental fields in the gauge theory. \mathcal{E} can roughly be thought of as a basis of branes.

An important feature of exceptional collections for us will be the ordering. The ordering of a collection induces an ordering of the nodes of the quiver. In order to use the exceptional collection technology to compute the beta functions, we must keep track of the ordering.

If a given quiver satisfies the well split condition of [11], the order of the quiver changes in a simple way under Seiberg duality. To understand the well split condition, we

first need to refine our understanding of the quiver ordering. It was shown in [11] that the ordering of the quiver is only determined up to cyclic permutations. If $123 \dots n$ is a good ordering, then so is $23 \dots n1$. If a quiver is well split, then we can find a cyclic permutation such that for any node j , all the outgoing arrows from j go to nodes $i < j$ and all the in-going arrows into j come from nodes $i > j$. After a Seiberg duality on node j , j would become the last node in the quiver.

An unproven conjecture of [11] is that the Seiberg dual of a well split quiver is again well split. The conjecture was proven for four node quivers in [11] and no counterexamples are known to the authors. An appropriate understanding of ill split quivers is still lacking. For example, the correct determination of R-charges for them is still open [11]. Indeed, the fractional Seiberg dualities encountered in [21] may be problematic precisely for this reason. As our examples in the subsequent sections involve only Seiberg dualities of well split, four node quivers, we can be confident in our calculations.

In light of the exceptional collection language, we shall also make use of the matrix S which is an upper triangular matrix with ones along the diagonal and related to f_{ij} by

$$S_{ij} = \begin{cases} f_{ij} - f_{ji}, & i < j, \\ 1, & i = j, \\ 0, & i > j, \end{cases} \quad (2.6)$$

where we have assumed an ordering. The components S_{ij} , $i \neq j$, are still the number of arrows from node i to node j , except that now a negative entry corresponds to reversing the arrow direction. We will find it convenient to use a matrix \mathcal{I} which is simply the antisymmetrized version of S (or f)

$$\mathcal{I} = S - S^t = f - f^t. \quad (2.7)$$

Using this, chiral anomaly cancellation can be concisely expressed as the condition that the dimension vector d be in the kernel of \mathcal{I} . In other words, r and the s_i form a basis of $\ker \mathcal{I}$.

1. Beta functions and flows

Methods exist in the literature for the determination of the R-charges as well as the beta function. Evaluating Eq. (2.2) with the quiver notation introduced above, and denoting by R_{ij} the R-charge of the bifundamental X_{ij} , one obtains for the beta function of the i -th node [cf. Eq (5.7) of [5]]

$$\frac{dx_i}{d \ln \mu} = \beta_i = \left(3d^i + \frac{3}{2} \sum_{j=1}^k (f_{ij}(R_{ij} - 1) + f_{ji}(R_{ji} - 1))d^j \right), \quad (2.8)$$

where x_i is related to the i -th gauge coupling via $x_i \equiv 8\pi^2/g_i^2$.

One very insightful approach for the determination of the R-charge is the procedure of maximization of the central charge a in the CFT as advocated in [6,7]. We shall however adhere to the procedure of [11,12], which gives the

R-charges at the conformal point. Transcribing Eq. 49 from [12] to present notations, the R-charge of the bi-fundamental X_{ij} is given by

$$R(X_{ij}) = 1 + \left(\frac{2}{(9-n)r^i r^j} (S_{ij}^{-1} + S_{ji}^{-1}) - 1 \right) \text{sgn}(i-j). \quad (2.9)$$

It was shown in [12] that plugging Eq. (2.9) into Eq. (2.8), and going to the conformal point $d^i = r^i$, one finds $\beta_i = 0$, as expected.

The flow is induced when we leave the conformal fixed point by adding D5-branes. As in [3], we will work in the regime $M^I \ll N$. We will assume the R-charges do not receive corrections of $\mathcal{O}(M^I/N)$. This assumption is supported by the supergravity solutions we write down in Sec. V, which severely constrain the nature of such corrections for KS type cascades. For more general cascades with duality walls, we believe that we can still trust the qualitative nature of our results. Ignoring the corrections, the nonconformal beta functions can readily be obtained by substituting Eq. (2.9) into Eq. (2.8) for general ranks d^i . We obtain, to order M^I/N ,

$$\beta_i = 3s_i^i M^I + \frac{3}{2} \sum_j \tilde{R}_{ij} s_j^j M^I, \quad (2.10)$$

where we have introduced the symmetric matrix

$$\tilde{R}_{ij} = f_{ij}(R_{ij} - 1) + f_{ji}(R_{ji} - 1). \quad (2.11)$$

We will now evolve the inverse gauge couplings $x_i = 8\pi^2/g_i^2$ with the beta functions (2.10). Since the one-loop beta functions are constant, the evolution proceeds in step-wise linear fashion, much like the KS cascade; we have

$$\frac{8\pi^2}{g_i^2(t+\Delta t)} - \frac{8\pi^2}{g_i^2(t)} = \beta_i \Delta t \quad (2.12)$$

during the step Δt in energy scale ($t = \ln \mu$), before one has to perform Seiberg duality on the node whose coupling reaches zero first.

An important constraint can be placed on this evolution. Even though now these beta functions do not vanish identically, it is still the case that

$$\sum_i^k \beta_i r^i = 0. \quad (2.13)$$

The reason is that this sum can be reorganized into a sum over each of the beta functions at the conformal point, and at the conformal point, each of these beta functions vanishes individually. It follows from Eqs. (2.10) and (2.13), therefore, that

$$\sum_i^k \frac{r^i}{g_i^2} = \text{const} \quad (2.14)$$

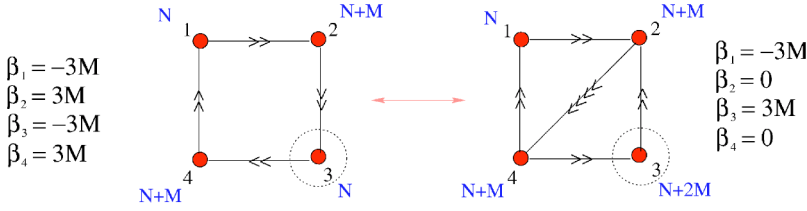


FIG. 2. The first class of duality cascades for F_0 . This is an immediate generalization of the KS conifold case and we alternate between the two theories upon dualizing node 3 of each and evolve according to the beta functions shown.

throughout the course of the cascade; on this constraint we shall expound next.

2. Simplices in the space of couplings

The space of possible gauge coupling constants $x_i \equiv 1/g_i^2$ for a quiver with k gauge groups is a cone $(\mathbb{R}_+)^k$. The relation (2.14) cuts out a *simplex* in this cone. The beta functions (2.10) establish the direction of the renormalization group flow inside this simplex. For the KS conifold flow, having two gauge couplings, the cone is the quadrant in \mathbb{R}^2 parametrized by $1/g_1^2 = x > 0$ and $1/g_2^2 = y > 0$. The simplex is the line segment $x + y = \text{const}$ inside this cone. The beta functions tell us to move up and down this line segment until one or the other coupling constant diverges.

In more general cases, under the renormalization group flow, we will eventually reach a face of the simplex where one of the couplings diverges. At this point, the insight gained from the KS flow tells us we should Seiberg dualize the corresponding gauge group. After the duality, we find ourselves typically in a new gauge theory. The new gauge theory has some new associated simplex and renormalization group flow direction given by some different set of beta functions. The KS flow is very special in that the Seiberg dual theory is identical to the original one up to the total number of D3-branes N .

One imagines in general some huge collection of simplices glued together along their faces. In any given simplex, the renormalization group trajectory is a straight line. At the faces, the trajectory “refracts.” One recomputes the beta functions to find the new direction for the RG flow. In Fig. 1 for example, we have the evolution of the couplings reflecting off the t -axis (corresponding to either $1/g_1^2$ or $1/g_2^2$ equal to zero), whereby giving the weave pattern. Note that such RG flows are generically quite sensitive to initial conditions. Slightly altering the initial couplings may alter the trajectory such that a different face of a simplex is reached. A different face corresponds to a Seiberg duality on a different node which will generically completely alter the rest of the flow. Such a sensitivity was noticed in [4,5].

For four node quivers, the simplices are tetrahedra and the RG flow can be visualized. There is only one vector s , with components s_i , corresponding to only one D5-brane. Thus, the direction of the RG flow inside any given tetrahedron is, up to sign, independent of M . Moreover, one can show that after a duality on node i , $\beta_i \rightarrow -\beta_i$ (see the Appendix for details).

Thus prepared, we can embark upon a detailed study of the RG flows and duality cascades for various concrete examples. Some of them will exhibit a KS type behavior, meaning that the cascade will periodically return to the same

quiver up to a change in the number of D3-branes, showing no accumulation of dualization scales in the UV. Others will be markedly different, exhibiting duality walls. In particular, we shall describe an assortment of interesting flows for D-branes probing cones over the del Pezzo surfaces, where we will be able, in addition to numerics, to gain some quantitative analytic understanding.

III. DUALITY WALLS FOR F_0

We begin with D-brane probe theories on the complex cone over F_0 , the zeroth Hirzebruch surface. The addition of D5-branes takes us out of conformality, whereby inducing a RG flow. Detailed numerical study was undertaken in [5]. All Seiberg dual theories for this geometry can be arranged into a web which encodes all possible duality cascades. This web takes the form of a flower and has been affectionately called the *Flos Hirzebruchiensis* (cf. Fig. 7 cit. *ibid.*). The purpose of this section is to derive analytical results for the existence of duality walls and their location. We also explain the *fractal structure* of the duality wall curve as a function of the initial couplings.

A. Type A and type B cascades

Before proceeding with the analytical derivations, let us make a brief summary of the findings in [5], where two classes of RG trajectories were identified. In one gauge theory realization, F_0 exhibits a Klebanov-Strassler type flow that alternates between two quivers with constant intervals in $t = \log \mu$ (for energy scale μ) between successive dualizations. This type of flow is an immediate generalization of the conifold cascade. The quivers of and the beta functions inter-connecting between the two theories are shown in Fig. 2.

The second class of flows commences with the quiver in Fig. 3, which is another theory in the duality flower for F_0 .

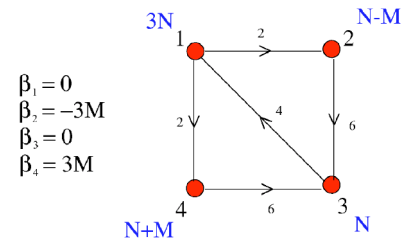


FIG. 3. The second class of theories for F_0 . Starting from this quiver and following the duality cascade give markedly different behavior from the KS case. It was seen in this case that the increment in energy scale decreases at each step and a “duality wall” may be reached [5].

In this case, there is a decrease in the t interval between consecutive dualizations towards the UV, leading to the possibility of a so-called “duality wall” past which no more dualization is possible and we have an accumulation point at finite energy. Considering initial couplings of the four gauge group factors of the form $(1, x_2, x_3, 0)$, two qualitatively different behaviors were observed.

- (1) In theories with $x_3 > 0.9$, the cascade corresponds to an infinite set of alternate dualizations of nodes 1 and 2. The distance between dualizations is monotonically decreasing, as was shown in Figs. 12 and 13 of [5]. However, no conclusive evidence of convergence to a duality wall was found therein. We will call such a cascade an *A type cascade* and will show shortly that in this case a duality wall is indeed approached smoothly.
- (2) On the other hand, for $x_3 < 0.9$, the third gauge group is dualized at a finite scale. When this happens, all the intersection numbers in the quiver become larger than 2, leading to an explosive growth of the ranks of the gauge groups and the number of bifundamental chiral fields, and generating an immediate accumulation of the dualization scales. This discontinuous behavior makes duality walls evident even in numerical simulations for these flows. We will refer to these flows as *B type cascades*.

B. Duality walls in type A cascade

Having elucidated the rudiments of the cascading behavior of the F_0 theories, let us explore whether there are indeed duality walls for A type cascades, which we recall to be the type for which numerical evidence is not conclusive. We shall proceed analytically. In order to do so, let us first construct the quiver at an arbitrary step k . We can regard Seiberg duality as a matrix transformation on the rank vector and the adjacency matrix as was done for example in Sec. 8.1 of [5]. An elegant way to derive the quiver at a generic position in the cascade is by realizing Seiberg duality transformations as mutations in an exceptional collection (equivalently, by Picard-Lefschetz monodromy transformations on the 3-cycles in the manifold mirror to the original Calabi-Yau). We will use this language as was done in [11,12].

Taking the exceptional collection to be $(a, b, 3, 4)$, the alternate dualizations of nodes 1 and 2 corresponds in this language to the repeated left mutation of a with respect to b . For even k $(a, b) = (1, 2)$, while for odd k $(a, b) = (2, 1)$. Figure 3 corresponds to $k=1$ where the exceptional collection ordering is $(2, 1, 3, 4)$. This quiver is well split.

1. Quivers at step k

Under Seiberg duality, the rank of the relevant gauge group changes from N_c to $N_f - N_c$. Type A cascades correspond to always dualizing node a . By explicitly constructing these RG trajectories, we will check that this assumption is indeed consistent. The exceptional collection tells us that after the duality, nodes a and b will switch places. Thus

$$\begin{aligned} N_a(k+1) &= N_b(k), \\ N_b(k+1) &= 2N_b(k) - N_a(k). \end{aligned} \quad (3.1)$$

It is immediate to prove that after k iterations, the ranks of the $SU(N_i)$ gauge groups are given by

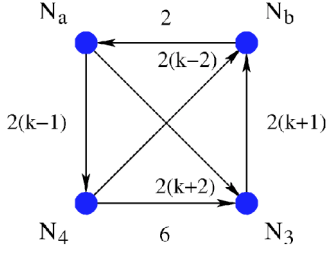
$$\begin{aligned} N_a &= (2k-1)N + (k-2)M, \\ N_b &= (2k+1)N + (k-1)M, \\ N_3 &= N, \\ N_4 &= N + M. \end{aligned} \quad (3.2)$$

The number of bifundamental fields between each pair of nodes follow from applying the usual rules for Seiberg duality of a quiver theory. In particular, we combine the bifundamentals X_{a4} , X_{ba} , and X_{a3} into mesonic operators $M_{b4} = X_{ba}X_{a4}$ and $M_{b3} = X_{ba}X_{a3}$. We introduce new bifundamentals X'_{4a} , X'_{ab} , and X'_{3a} with dual quantum numbers along with the extra term $M_{b4}X'_{4a}X'_{ab} + M_{b3}X'_{3a}X'_{ab}$ to the superpotential. We then use the superpotential to integrate out the massive fields, which appear in the quiver as bidirectional arrows between the pairs of nodes $(3, b)$ and $(4, b)$. The resulting incidence matrix for the quiver will change such that

$$\begin{aligned} f_{ba}(k+1) &= f_{ba}(k) & f_{3b}(k+1) &= f_{a3}(k) & f_{43}(k+1) &= f_{43}(k) \\ f_{a4}(k+1) &= -f_{4b}(k) + 2f_{a4}(k) & f_{4b}(k+1) &= f_{a4}(k) & f_{a3}(k+1) &= -f_{3b}(k) + 2f_{a3}(k) \end{aligned} \quad (3.3)$$

which can be simplified to yield

$$\begin{aligned} f_{ba}(k) &= 2 & f_{3b}(k) &= 2(k+1) & f_{43}(k) &= 6 \\ f_{a4}(k) &= 2(k-1) & f_{4b}(k) &= 2(k-2) & f_{a3}(k) &= 2(k+2). \end{aligned} \quad (3.4)$$

FIG. 4. Quiver diagram at step k of a type A cascade for F_0 .

This information can be summarized in the quiver diagram in Fig. 4.

With the adjacency matrix (3.4) and the nonconformal ranks (3.2), we can readily compute the beta functions from Eq. (2.10), to arrive at

$$\begin{aligned}
 \beta_a &= -\frac{9(k+1)kM}{(4k+2)} < 0 \\
 \beta_b &= \frac{9(k-1)kM}{(4k-2)} \geq 0 & k=1,2,3,\dots \\
 \beta_3 &= \frac{3(7k^2-3k-4)M}{(2-8k^2)} < 0 & (a,b)=(2,1), \text{ } k \text{ odd,} \\
 \beta_4 &= \frac{3(7k^2+3k-4)M}{(-2+8k^2)} > 0, & (a,b)=(1,2), \text{ } k \text{ even.}
 \end{aligned} \tag{3.5}$$

2. The RG flow

Using the results in Sec. III B 1, we proceed to study the evolution of the dualization scales starting with the initial couplings $(1, x_2(0), x_3(0), 0)$. Let us consider the first step in the cascade. We are in a type A cascade, so $x_3(0) > 0.9$. The beta functions are, from Eq. (3.5),

$$\beta_1(1)=0, \quad \beta_2(1)=-3M, \quad \beta_3(1)=0, \quad \beta_4(1)=3M. \tag{3.6}$$

We see that only node 2 has a negative beta function at the first step and so its associated coupling will reach zero first, i.e., the first step ends with the dualization of node 2. The subsequent increment $\Delta(1)$ in the energy scale $t = \log \mu$ before the dualization is performed is equal to

$$\Delta(1) = \frac{x_2(0)}{|\beta_2(1)|}. \tag{3.7}$$

Applying

$$\begin{aligned}
 x_i(k+1) &= x_i(k) + \beta_i(k+1)\Delta(k+1), \\
 t(k+1) &= t(k) + \Delta(k),
 \end{aligned} \tag{3.8}$$

we have at the end of this step

$$x_1(1)=1, \quad x_2(1)=0, \quad x_3(1)=x_3(0), \quad x_4(1) = \frac{3Mx_2(0)}{|\beta_2(1)|}. \tag{3.9}$$

So, as far as nodes 2 and 3 are concerned, the initial value $x_2(0)$ only affects the length of the first step, beyond which any information about it is erased. In order to look for the initial couplings that lead to a type A flow, recall that we have to determine the possible initial values $x_3(0)$ such that $x_3(k)$ remains greater than zero as $k \rightarrow \infty$ so that the third node never becomes dualized. Since $\beta_3(1)=0$, this is completely independent of $\Delta(1)$ and hence independent of $x_2(0)$.

That said, let us look at the cascade at the next step. The beta functions (3.5) now give

$$\begin{aligned}
 \beta_1(2) &= -\frac{27}{5}M, \quad \beta_2(2)=3M, \quad \beta_3(2)=-\frac{9}{5}M, \\
 \beta_4(2) &= 3M.
 \end{aligned} \tag{3.10}$$

Since we are interested in type A cascades, we assume that the initial value $x_3(0)$ is such that this node is never dualized. Thus, the next node to undergo Seiberg duality is the other one with a negative beta function, namely node 1. Recalling that $x_1(1)=1$, the consequent step in the energy scale $\Delta(2)$ is thus

$$\Delta(2) = \frac{x_1(1)}{|\beta_1(2)|} = \frac{1}{|\beta_1(2)|}, \tag{3.11}$$

and $x_1(2)=0$ while $x_2(2)=\beta_2(2)\Delta(2)$. Proceeding similarly, the next step gives

$$\Delta(3) = \frac{\beta_2(2)}{\beta_1(2)} \frac{1}{\beta_2(3)}. \tag{3.12}$$

We see that in general, at the k^{th} step, the interval $\Delta(k)$ is given by

$$\Delta(k) = \left[\prod_{i=2}^k \frac{\beta_b(i)}{|\beta_a(i)|} \right] \frac{1}{\beta_b(k)}, \quad \begin{aligned} &(a,b)=(2,1), \quad k \text{ odd,} \\ &(a,b)=(1,2), \quad k \text{ even,} \end{aligned} \tag{3.13}$$

for $k \geq 2$. This, using Eq. (3.5), can be written as a telescoping product

$$M\Delta(k) = \left[\prod_{i=2}^k \frac{(i-1)}{(i+1)} \frac{(2i+1)}{(2i-1)} \right] \frac{(4k-2)}{9(k-1)k}. \tag{3.14}$$

Simplifying this expression we arrive at

$$M\Delta(k) = \frac{2(2k+1)(4k-2)}{27k^2(k^2-1)} \tag{3.15}$$

for $k \geq 2$. The total variation of the third coupling x_3 , after k steps, is given by

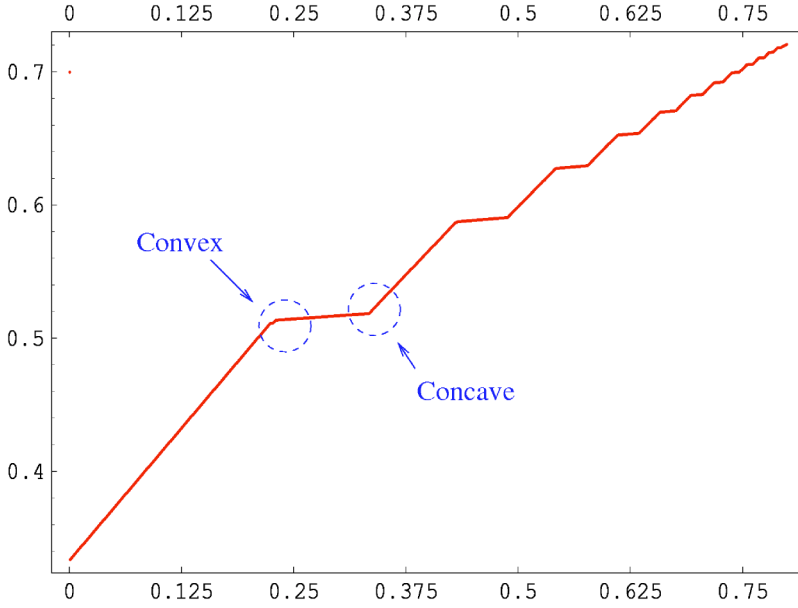


FIG. 5. Position of the duality wall for F_0 as a function of $x_3(0)$ for initial conditions of the form $(1, 1, x_3(0), 0)$. A piecewise linear structure is seen for the type B cascade region, i.e., $x_3(0) < x_{3b} \sim 0.9$.

$$x_3(k) - x_3(0) = \sum_{i=2}^k \Delta(i) \beta_3(i). \quad (3.16)$$

As discussed, the boundary between type A and B cascades corresponds to initial conditions such that $x_3(k) \rightarrow 0$ for $k \rightarrow \infty$, i.e., the initial conditions that separate the regime in which node 3 gets dualized at some finite k from the one in which it never undergoes a Seiberg duality. Then,

$$x_3(0) - x_3(\infty) = \frac{2}{9} \sum_{i=2}^{\infty} \frac{(7i+4)}{i^2(i+1)} = \frac{4}{27} \pi^2 - \frac{5}{9}. \quad (3.17)$$

We see that this sum is approximately equal to 0.906608, in agreement with the numerical evidence, which located the transition at $x_3(0) \sim 0.9$. We will henceforth call this coupling $x_3(0)$ such $x_3(\infty) = 0$, x_{3b} , because it is a boundary value between type A and type B cascades.

3. Duality walls in type A cascades

The computations in the previous section enable us to address one of the questions left open in [5], namely whether duality walls exist in this case. Our flow, from Eq. (3.17), corresponds to an infinite cascade that only involves nodes 1 and 2. Let us sum up all the steps $\Delta(k)$ in the energy scale *ad infinitum*; this is equal to

$$\sum_{k=1}^{\infty} \Delta(k) = \Delta(1) + \sum_{k=2}^{\infty} \Delta(k). \quad (3.18)$$

Using $\Delta(1) = x_2(0)/|\beta_2(1)| = x_2(0)/3M$ and Eq. (3.15), we see that this sum can actually be performed, giving us a finite answer. This means that there is indeed a duality wall for our type A cascades, whose value is equal to

$$t_{\text{wall}} = \frac{1}{3M} \left(x_2(0) + \frac{2\pi^2}{27} + \frac{5}{9} \right). \quad (3.19)$$

We would like to emphasize that, although derived in the approximation of vanishing $\mathcal{O}(M/N)$ corrections to the R-charges, Eq. (3.19) is the first analytical result for a duality wall. Given the detailed understanding we have of every step of the cascade on the gauge theory side, this example stands as a natural candidate in which to try to look for a realization of this phenomenon in a SuGRA dual.

C. Fractal structure of the duality wall curve

Having analytically ascertained the existence and precise position of the duality wall for type A cascades, and the boundary value $x_{3b}(0)$ of the inverse squared coupling at which the cascades become type B, we now move on to address another fascinating question, hints of which were raised in [5,12], viz., the dependence of the position of the wall upon the initial couplings. We will see that, in type B cascades, such dependence takes the form of a *self-similar* curve.

Let us focus on the one dimensional subset of the possible initial conditions given by couplings of the form $(1, 1, x_3(0), 0)$ (more general initial conditions can be studied in a similar fashion). Figure 5 is a plot of the position of the duality wall as a function of $x_3(0)$. Initial values $x_3(0) > x_{3b}$ correspond to type A cascades. Node 3 is not dualized in this case and thus the position of the wall is independent of $x_3(0)$ in this range, as determined by Eq. (3.19). From now on, we will focus on the $x_3(0) < x_{3b}$ type B region. The curve exhibits in this region an apparent piecewise linear structure as was noticed in [5].

In order to appreciate the piecewise structure more clearly, it is useful to consider the derivative of the curve. We show in Fig. 6 a numerical differentiation of Fig. 5. This apparent linearity is in fact approximate, and an intricate structure is revealed when we look at the curve in more detail. While exploring the origin of the different features of the curve, we will discover that a *self-similar fractal structure* emerges.

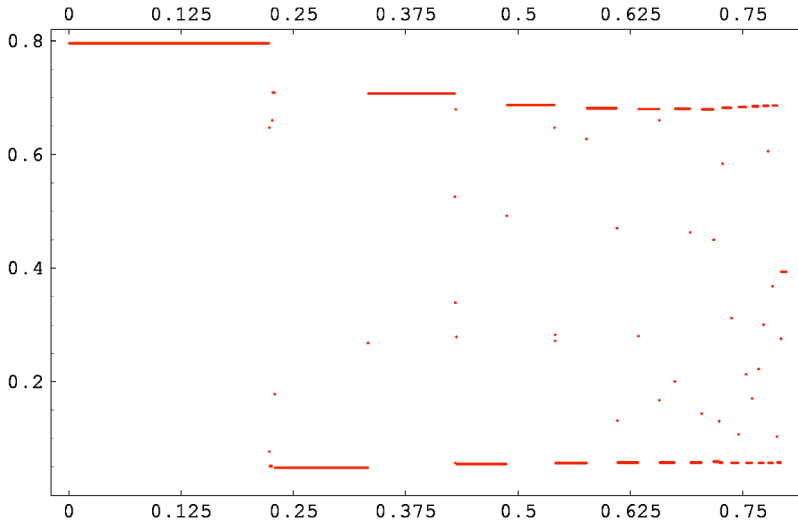


FIG. 6. Derivative of the position of the duality wall for F_0 as a function of $x_3(0)$ for initial conditions of the form $(1, 1, x_3(0), 0)$. The appearance of the constant segments evidences further the piecewise linear behavior of position of the wall with respect to $x_3(0)$.

The most prominent features in Fig. 5 are the *concave* and *convex cusps* at the end points of apparently linear intervals. In our notation (cf. figure), the bend at ≈ 0.2 is a convex cusp while the one at ≈ 0.3 is a concave one. We will explain now their origin and give analytical expressions for their positions.

As we will illustrate with examples, this kind of structure appears at those values of the couplings at which a transition between different cascades occurs. A semi-quantitative measure of how different two cascades are is given by the number of steps m that they share in common. In this sense, if a given cascade A shares m_1 steps with cascade B and m_2 with cascade C, with $m_1 > m_2$, we say that A is closer to B than to C. The general principle is that the closer the cascades between which a transition occurs at a given initial coupling, the smaller the corresponding feature in the position of duality wall versus coupling curve is.

It is important to remember what the physical meaning of our computations is. Numbering cascade steps increasing towards the UV and identifying the values of the initial couplings are just a simple way to handle the process of reconstructing a duality cascade. This cascade represents a traditional RG flow in the IR direction, in which Seiberg duality is used to switch to alternative descriptions of the theory beyond infinite coupling. At some stage of this flow in the IR the model in Fig. 3 appears, with couplings given precisely by what we called initial conditions. Thus, two cascades that share a large number of steps m in common, correspond to two RG flows initiated at different theories with large gauge groups and number of bifundamental fields in the UV that converge at some point, sharing the last m steps prior to reaching the model in Fig. 3. Due to the fact that a duality wall exists, the independent flows before convergence of the cascades take place in a very small range of energies.

We now investigate the convex and concave cusps of the curve. Our approach consists of identifying what happens to the cascades at those special points, and then computing the corresponding values of the initial couplings analytically. Let us first consider the *concave cusps*. The m -th concave cusp corresponds to the transition from node 3 being dualized at

step $m+1$ to it being dualized at step $m+2$. The cascades at both sides of the m -th concave cusp share the first m steps and are of the form

$$\begin{array}{c} 2121 \dots a3 \\ \underbrace{2121 \dots ab3}_m \end{array} \quad (3.20)$$

where $(a, b) = (1, 2)$ for m even and $(2, 1)$ for m odd. In this way, concave cusps fit in our general discussion of transitions between cascades, and we see that cusps become smaller as m is increased. The values of $x_3(0)$ that correspond to the concave cusps are obtained by setting $x_3(k) = 0$ in Eqs. (3.16) and (3.17) for $k \geq 2$, i.e.,

$$x_3^{conc}(k) = \frac{2}{9} \sum_{i=2}^k \frac{(7i+4)}{i^2(i+1)}, \quad k \geq 2. \quad (3.21)$$

From Eq. (3.21), the first concave cusps are located at $x_3(0)$ equal to

$$\frac{1}{3}, \quad \frac{79}{162}, \quad \frac{467}{810}, \quad \frac{2569}{4050}, \quad \frac{19133}{28350}, \dots \quad (3.22)$$

in complete agreement with the numerical values of Figs. 5 and 6.

Let us move on and study the convex cusps in Fig. 5. In analogy with Eq. (3.20), we claim that the m th convex cusp corresponds to cascades switching between

$$\begin{array}{c} 2121 \dots a3a \\ \underbrace{2121 \dots a3b}_m \end{array} \quad (3.23)$$

with $(a, b) = (1, 2)$ for m even and $(2, 1)$ for m odd. In order to check whether the proposal in Eq. (3.23) is correct, we proceed to compute the positions for the cusps that it predicts. The calculation is similar to the one in Sec. III B 2 and we only quote its result here

$$x_3^{conv}(k) = \frac{(4+7k)(10+49k+50k^2+14k^3)}{9k^2(1+k)^2(3+22k+14k^2)} + \frac{2}{9} \sum_{i=2}^{k-1} \frac{(7i+4)}{i^2(i+1)}, \quad k \geq 2. \quad (3.24)$$

Equation (3.21) determines the following positions for the first convex cusps

$$\frac{70}{309}, \frac{21773}{50544}, \frac{76733}{141750}, \frac{457831}{750060}, \frac{83386559}{126809550}, \dots \quad (3.25)$$

which are in perfect accordance with Figs. 5 and 6, whereby validating Eq. (3.23).

The fractal. Something fascinating happens when the duality wall curve is studied in further detail. Although convex cusps appear as such when looking at the curve at a relatively small resolution as in Fig. 5, an infinite fractal series of concave and convex cusps blossoms when we zoom in further and further. As an example, we show in Fig. 7 successive amplifications of the area around the first convex cusp, indicating the dualization sequences associated to each side of a given cusp. According to our previous discussion, this cusp is located at $x_3(0) = 70/309$ and corresponds to the transition between two cascades differing at the third step: $232 \dots$ and $231 \dots$. Figure 7(b) zooms in. We can appreciate that what originally seemed to be a convex cusp becomes a pair of convex cusps with a concave one in the middle. Furthermore, the value of $x_3(0)$ given by Eq. (3.24) is in fact the one that corresponds to this originally hidden concave cusp. The new convex cusps are of a higher order, corresponding to transitions between cascades at the 4th step. The first one in Fig. 7(b) corresponds to $2323 \dots \rightarrow 2321 \dots$ while the second one is associated to $2312 \dots$

$\rightarrow 2313 \dots$. We see in Fig. 7(c) how each of the convex cusps splits again into two 5th order convex cusps with a concave one in between.

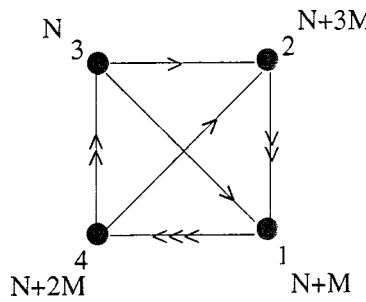
This procedure can be repeated indefinitely. We conclude that concave cusps are fundamental, while an infinite self-similar structure that corresponds to increasingly closer cascades can be found by expanding convex cusps.

IV. RG FLOWS AND QUASIPERIODICITY

Having expounded in detail the analytic treatment of RG flows for the zeroth Hirzebruch theory as well as their associated fractal behavior, let us move on to see what novel features arise for more complicated geometries. We recall the next simplest del Pezzo surface is the blow up of \mathbb{P}^2 at 1 point, the so-called dP_1 . The gauge theory for D3-brane probes on the cone over dP_1 was constructed via toric algorithms in [18]. There are infinitely many quiver gauge theories which are dual to this geometry. Their connections under Seiberg duality can be encoded in a duality tree. When D5-branes are included, the duality tree becomes a representation of the possible paths followed by a cascading RG flow. The tree for dP_1 appears in Fig. 18 of [5]. This tree contains isolated sets of quivers with conformal ranks $r = (1,1,1,1)$, denoted toric islands in [5]. We will find quasiperiodicity of the gauge couplings for RG cascades among these islands.

A. Initial theory

We are interested in studying the RG flow of a gauge theory corresponding to dP_1 . For simplicity, let us choose one of the dual quivers with a relatively small number of bifundamentals. Our quiver is described by the following (we have also included the inverse matrix as a preparation to compute the R-charges):



$$S = \begin{pmatrix} 1 & -2 & -1 & 3 \\ 0 & 1 & -1 & -1 \\ 0 & 0 & 1 & -2 \\ 0 & 0 & 0 & 1 \end{pmatrix}, \quad S^{-1} = \begin{pmatrix} 1 & 2 & 3 & 5 \\ 0 & 1 & 1 & 3 \\ 0 & 0 & 1 & 2 \\ 0 & 0 & 0 & 1 \end{pmatrix}. \quad (4.1)$$

We start with a gauge theory with N D3-branes and M D5-branes, $M \ll N$, corresponding to gauge groups

$$SU(N+M) \times SU(N+3M) \times SU(N) \times SU(N+2M). \quad (4.2)$$

Chiral anomaly cancellation is satisfied since the D3-brane vector $r = (1,1,1,1)$ and the D5-brane vector $s = (1,3,0,2)$ are

in the kernel of $S - S^T$. In fact, the kernel of $S - S^T$ is two dimensional, and these are the only kinds of D-branes that are allowed. The R-charges of the bifundamental fields at the conformal point are then, using Eq. (2.9),

$$R(X_{32}) = \frac{1}{4},$$

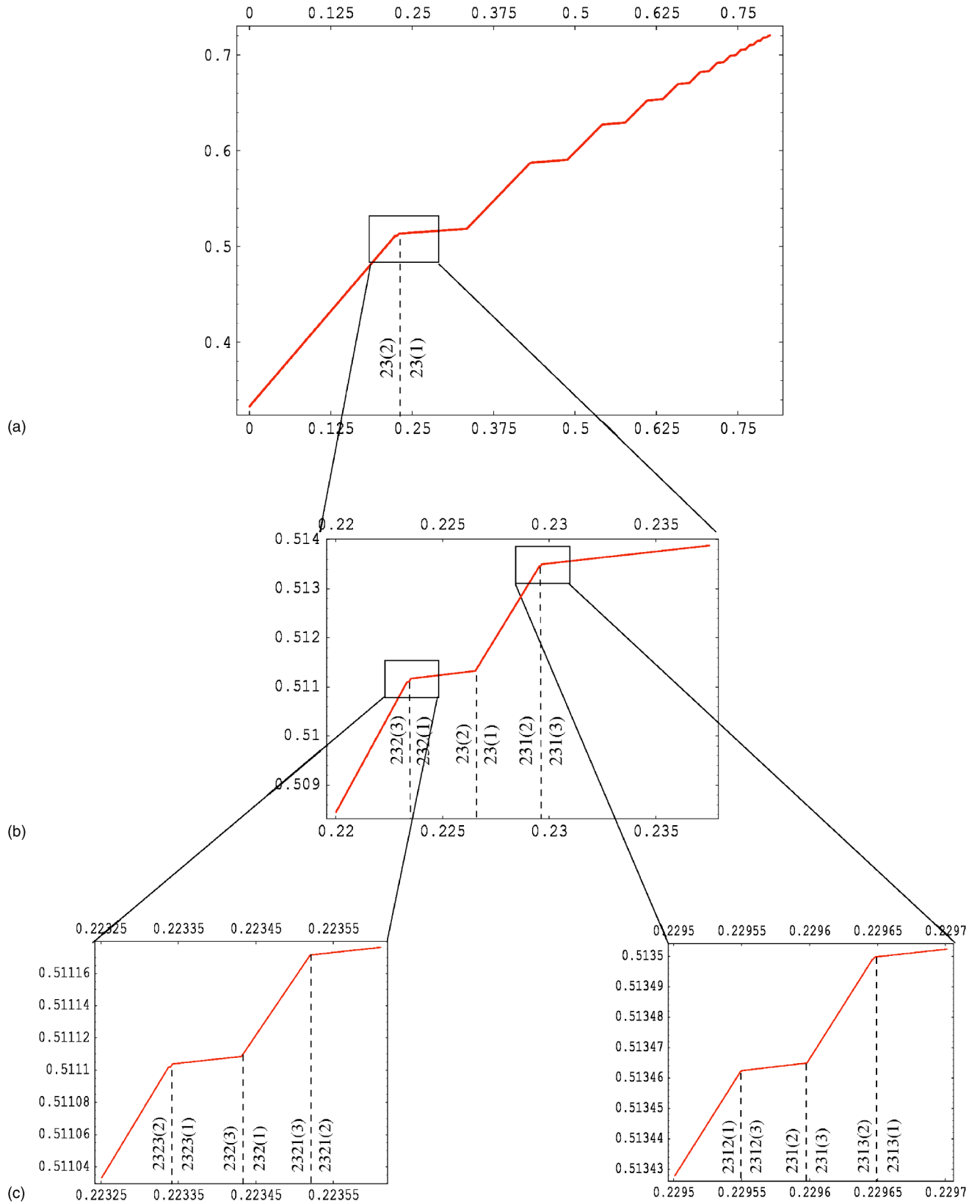


FIG. 7. Successive amplifications of the regions around convex cusps show the self-similar nature of the curve for the position of the wall versus $x_3(0)$. We show the first steps of the cascades at each side of the cusps, indicating between parentheses the first dualizations that are different.

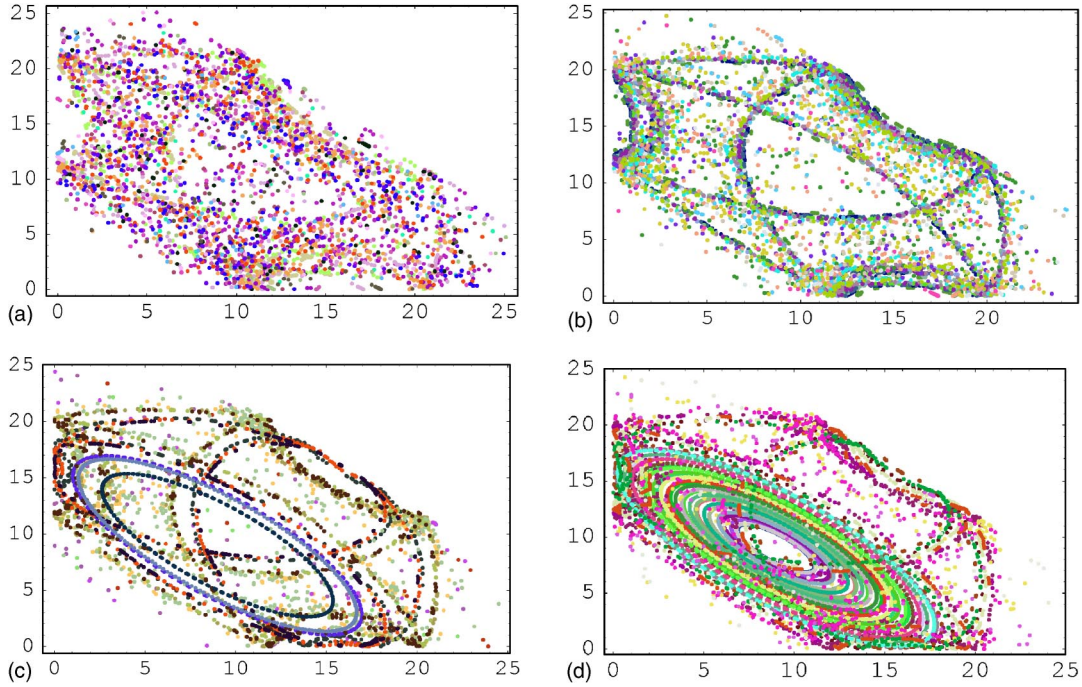


FIG. 8. Scatter plot of (x_3, x_4) that are nonzero during 800 dualization steps for the initial value $(32 - x_3(0) - x_4(0), 0, x_3(0), x_4(0))$. In each plot, $(x_3(0), x_4(0))$ is allowed to range over a rectangular region with lower left corner L , upper right corner R , and minimum step size in the $x_3(0)$ and $x_4(0)$ directions equal to δ_3 and δ_4 respectively. (a) $L = (9, 15\frac{7}{8})$, $R = (10, 16\frac{2}{8})$, $\tilde{\delta} = (\frac{1}{4}, \frac{1}{8})$; (b) $L = (9, 15\frac{3}{8})$, $R = (10, 15\frac{6}{8})$, $\tilde{\delta} = (\frac{1}{4}, \frac{1}{8})$; (c) $L = (2, 6)$, $R = (5, 9)$, $\tilde{\delta} = (1, 1)$; (d) $L = (7, 11)$, $R = (9, 17)$, $\tilde{\delta} = (1, \frac{1}{2})$. We use a different color for every set of initial conditions.

$$R(X_{21}) = R(X_{43}) = \frac{1}{2},$$

$$R(X_{42}) = R(X_{31}) = R(X_{14}) = \frac{3}{4}. \quad (4.3)$$

As before, we assume the conformal R-charges get corrections only at order $(M/N)^2$. Subsequently, using Eq. (2.10) we calculate the one loop beta functions for the four gauge groups to be

$$\beta/M = (-15/4, 27/4, -27/4, 15/4). \quad (4.4)$$

B. RG flow

As discussed above, we let the gauge couplings evolve according to the beta functions and we perform a Seiberg duality on the gauge group factor whose coupling diverges first. Interestingly, a Seiberg duality on node 2 or 3 produces the same quiver up to permutation (with the rank of the dualized gauge group appropriately modified). On the other hand, Seiberg duality on nodes 1 or 4 produces a different quiver with larger numbers of bifundamentals.

In the next section, we will perform a numerical study of the possible flows. We will see how certain RG flows involve a single type of quiver and periodically return to the starting point up to a change in the number of D3-branes. These cases are the dP_1 analogues of the KS cascade. We will also discover other more intricate flows with a beautiful structure,

depending on the initial conditions. We will describe the KS type flows analytically in Sec. IV B 2.

1. Poincaré orbits

Let us explore the two-dimensional space of initial couplings $(c - x_3(0) - x_4(0), 0, x_3(0), x_4(0))$, where c is some constant that fixes the overall normalization. Next, choose some initial value for the pair $(x_3(0), x_4(0))$ and evolve the cascade for a large number of steps. An interesting way of visualizing these flows is the following. We keep all the values of (x_3, x_4) which are both nonzero, i.e., when either node 1 or 2 but neither node 3 nor 4 is dualized. A subsequent scatter plot can be made for these values, and is presented in Fig. 8 for various choices of initial conditions, which are identified by different colors.

We see different types of behavior according to the initial conditions. First, there are elliptical trajectories. They correspond to cascades that only involve $r = (1, 1, 1, 1)$ quivers. In the language of [5], the entire RG flow takes place within a single toric island. The next section will be devoted to a detailed study of this case. Other trajectories jump among three squashed ellipses. These cascades consist of both quivers with $r = (1, 1, 1, 1)$ and $r = (2, 1, 1, 1)$ (and its permutations) and correspond to hopping around the six toric islands. Finally, other flows have a diffuse scatter plot, and correspond to cascades that travel to quivers with arbitrarily large gauge groups. Outside the stable elliptical orbits, numerically we find sensitive dependence on the initial conditions.

The scatter plots are reminiscent of the Poincaré surface-of-section (SoS) plots used in the study of chaotic dynamics.

We recall that a Poincaré SoS is a surface in phase space which cuts the trajectory of a system. If the trajectory is periodic or quasiperiodic, the accumulation of intersection points where the trajectory cuts the surface often produces cycles. In our case, instead of phase space, the RG cascade is a trajectory inside the space of couplings, which we recall from Sec. II B 2 to be a glued set of tetrahedra. The ellipses we observe are sections thereof. In the above plots, we have actually superimposed different surfaces, $x_2=0$ and $x_1=0$, but a symmetry has kept the picture from getting muddled.

2. Analytical evolution

Let us follow the RG flow analytically through several Seiberg dualities. We will focus on a particular sequence of dualities which repeats the sequence of dualizations on nodes 3, 1, 4 and 2. We will check later that this is indeed a consistent cascade that takes place once the initial conditions are chosen appropriately. This set of dualizations never changes the quiver, but merely amounts to a permutation of the nodes after each step. Furthermore, after four steps the cascade returns to the original quiver, with the same ordering of the nodes, but with the ranks changed as: $N_i \rightarrow N_i + 4M$.

Now we are ready to try to understand the regime of initial conditions which will allow for such a flow. Let the initial inverse gauge couplings be $x = (x_1, x_2, x_3, x_4)$ and set $M=1$. The change in couplings from four steps of Seiberg dualities (3142) can be cast as a linear operation sending $x \rightarrow \mathcal{M}x$ where \mathcal{M} is a 4×4 matrix:

$$\mathcal{M} = \begin{pmatrix} -55/729 & 5/9 & 6440/6561 & 56/81 \\ 0 & 0 & 0 & 0 \\ 154/729 & -5/9 & -1265/6561 & 70/81 \\ 70/81 & 1 & 154/729 & -5/9 \end{pmatrix}. \quad (4.5)$$

In particular, \mathcal{M} has eigenvectors

$$\lambda = 0, 1, \frac{-5983 \pm 1904i\sqrt{2}}{6561}. \quad (4.6)$$

The zero eigenvalue has eigenvector $v_0 = (-5, 9, -9, 5)$, which can be used to set $x_2=0$. The eigenvalue $\lambda=1$ has eigenvector $v_1 = (14, 0, 9, 9)$, and corresponds to a fixed point of the flow. If $x=v_1$, then the couplings will remain unchanged after a sequence of four Seiberg dualities. The normalization of this vector is the same one that was used in Fig. 8, where we can verify that the center of the ellipses is accordingly located at $(x_3, x_4) = (9, 9)$. Finally, the two complex eigenvalues, which we note to have unit modulus, and henceforth define to be

$$\lambda_{\pm} := e^{\pm i\theta}, \quad (4.7)$$

correspond to eigenvectors

$$v_{\pm} := \left(\frac{2}{3} e^{\pm i\alpha}, 0, e^{\pm i\beta}, 1 \right) \quad (4.8)$$

where

$$e^{i\alpha} = -\frac{1}{3} + \frac{2i\sqrt{2}}{3}, \quad e^{i\beta} = -\frac{7}{9} - \frac{4i\sqrt{2}}{9}. \quad (4.9)$$

Let us take our initial couplings to be $x = av_1 + cv_+ + c^*v_-$ for coefficients a and c . After a large number of Seiberg dualities, the couplings become, by Eq. (4.5),

$$x(n) = \mathcal{M}^n x = av_1 + c\lambda_+^n v_+ + c^*\lambda_-^n v_- . \quad (4.10)$$

The components of $x(n)$ are straightforwardly obtained, using the above expressions for the various eigenvalues, as

$$\begin{aligned} x_1 &= 14a + \frac{4}{3}|c|\cos(n\theta + \alpha + \delta) \\ x_2 &= 0 \\ x_3 &= 9a + 2|c|\cos(n\theta + \beta + \delta) \\ x_4 &= 9a + 2|c|\cos(n\theta + \delta) \end{aligned} \quad (4.11)$$

where we have set $c = |c|\exp(i\delta)$. We see that indeed, (x_3, x_4) give rise to the parametric equation for an ellipse with respect to the parameter n , in accord with the scatter plots (c) and (d) in Fig. 8. However, we must ask when is the above analysis applicable, i.e., when is our dualization sequence actually the sequence followed by the RG flow. Certainly a necessary condition is that the couplings x_1 , x_3 , and x_4 remain greater than zero during the flow. Thus, we see that $|c| < 9a/2$ with $a > 0$. Indeed, under the condition $|c| < 9a/2$, an elliptical disk in the coupling plane $x_2=0$ is traced. The boundary of the disk is an ellipse tangent to the $x_3=0$ and $x_4=0$ axes at the points $x/a = (16, 0, 0, 16)$ and $x/a = (16, 0, 16, 0)$. This condition also appears to be sufficient, as the numerics bear out. Initial conditions violating this condition will not generate ellipses, as demonstrated by plots (a) and (b).

Though one might worry, there is in fact no contradiction between this periodic behavior and the expectation that under RG flow, there will be fewer degrees of freedom in the IR than in the UV. This expectation has been encoded more precisely in the so-called a -conjecture (see for example [6] for a recent discussion). One can associate to any four-dimensional conformal theory a central charge denoted a which can be interpreted as a measure of the number of degrees of freedom in the theory. According to the a -conjecture, given UV and IR conformal fixed points, $a_{UV} > a_{IR}$. Now for our field theory analysis to be valid, our gauge theories should never be very far away from conformality, where this distance is measured by the $\mathcal{O}(M/N)$ corrections. One expects therefore that a can be loosely defined at any point in the RG cascade and moreover that a should be nonincreasing as we move into the IR. Recall that $a \sim \sum_{\psi} R(\psi)^3$ where the sum runs over the R-charges of all the fermions in the theory [22]. From the structure of these quiver theories, one sees that $a \sim N^2$ and moreover after a sequence of four dualities for the dP_1 flow above, $N \rightarrow N - 4M$. Thus a is indeed decreasing as we move into the IR despite the periodic behavior of the gauge couplings.

Increments in energy scale. One final question we can answer here is how does the RG scale grow along the flow. After a sequence of four Seiberg dualities, the RG scale changes by

$$\Delta t(n) = \frac{4}{27} \left(\frac{106}{81} x_1(n) + x_2(n) + \frac{1108}{729} x_3(n) + \frac{4}{9} x_4(n) \right). \quad (4.12)$$

In deriving this formula, we have had to look at the effect on the couplings of each of the four Seiberg dualities individually. The process is very similar to the calculations discussed in Sec. III B 2 and we will not repeat the details here. Using the results (4.11), one finds that

$$\Delta t(n) = \frac{16}{3} a + \frac{2^5 \times 7}{3^6} |c| \cos(n\theta + \delta + \gamma), \quad (4.13)$$

where

$$e^{i\gamma} = -\frac{241}{243} - \frac{22i\sqrt{2}}{243}. \quad (4.14)$$

Note that $\Delta t > 0$, but that t will have oscillations on top from the cosine:

$$t(n) = \frac{16}{3} an + \frac{2^5 \times 7}{3^6} |c| \frac{\cos(\delta + \gamma + n\theta/2) \sin((n+1)\theta/2)}{\sin(\theta/2)}. \quad (4.15)$$

The previous approach can be applied to periodic KS type cascades associated to other geometries. In the general case, as in the F_0 example of Fig. 2, more than one quiver can be involved in a period.

V. SUPERGRAVITY SOLUTIONS FOR DEL PEZZO FLOWS

In the above, we have discussed in detail the RG flows for some del Pezzo gauge theories from a purely field-theoretic point of view. This is only half of the story according to the AdS-CFT correspondence. It is important to find type IIB supergravity solutions that are dual to these field theory flows. As already emphasized [3], the main reason to trust that Seiberg duality cascades occur for the KS solution is not the field theory analysis but that it is reproduced by a well behaved supergravity solution. The purpose of this section is to investigate these dual solutions.

Surprisingly, even without a metric for the del Pezzos, we can demonstrate the existence of and almost completely characterize some of their supergravity solutions. The solutions we find are analogous to the Klebanov-Tseytlin (KT) solution [15] for the conifold. Recall that the KS solution is well behaved everywhere and asymptotes to the KT solution in the ultraviolet (large radius). The KT solution, on the other hand, is built not from the warped deformed conifold but from the conifold itself and thus has a singularity in the infrared (small radius).

A. Self-dual (2,1) solutions

To put these type IIB SuGRA solutions in historical context, note that they are closely related to a solution found by Becker and Becker [23] for M-theory compactified on a Calabi-Yau four-fold with four-form flux. One takes the four-fold to be a three-fold \mathbf{X} times T^2 and then T -dualizes on the torus, as was done in [24,25]. The crucial point here is that the resulting complexified three-form flux has to be imaginary self-dual and a harmonic representative of $H^{2,1}(\mathbf{X})$ to preserve supersymmetry. Graña and Polchinski [14] and also Gubser [26] later noticed that the KT and KS supergravity solutions were examples of these self-dual (2,1) type IIB solutions. [Indeed, the authors of [3] also mention that their complexified three-form is of type (2,1).]

Let us briefly review the work of Graña and Polchinski. The construction begins with a warped product of $\mathbb{R}^{3,1}$ and a Calabi-Yau three-fold \mathbf{X} :

$$ds^2 = Z^{-1/2} \eta_{\mu\nu} dx^\mu dx^\nu + Z^{1/2} ds_{\mathbf{X}}^2, \quad (5.1)$$

where the warp factor $Z = Z(p)$, $p \in \mathbf{X}$, depends on only the Calabi-Yau coordinates. We are interested in the case where \mathbf{X} is the total space of the complex line bundle $\mathcal{O}(-K)$ over the del Pezzo dP_n . Here K is the canonical class. The manifold \mathbf{X} is noncompact.

There exists a class of supersymmetric solutions with nontrivial flux

$$G_3 = F_3 - \frac{i}{g_s} H_3, \quad (5.2)$$

where $F_3 = dC_2$ is the RR three-form field strength and $H_3 = dB_2$ the NSNS three-form. To find a supergravity solution, the complex field strength G_3 must satisfy several conditions: G_3 must

- (1) be supported only in \mathbf{X} ;
- (2) be imaginary self-dual with respect to the Hodge star on \mathbf{X} , i.e., $\star_{\mathbf{X}} G_3 = i G_3$;
- (3) have signature (2,1) with respect to the complex structure on \mathbf{X} ; and finally,
- (4) be harmonic.

If these conditions are met, a supergravity solution exists such that the RR field strength F_5 obeys

$$dF_5 = -F_3 \wedge H_3, \quad (5.3)$$

and the warp factor satisfies

$$(\nabla_{\mathbf{X}}^2 Z) \text{vol}(\mathbf{X}) = g_s F_3 \wedge H_3, \quad (5.4)$$

where $\text{vol}(\mathbf{X})$ is the volume form on \mathbf{X} . In particular, $\text{vol}(\mathbf{X}) = r^5 dr \wedge \text{vol}(\mathbf{Y})$ where \mathbf{Y} is the (5 real-dimensional) level surface of the cone \mathbf{X} . The axion vanishes and the dilaton is constant: $e^\phi = g_s$.

B. (2,1) solutions for the del Pezzo

Let us construct such a G_3 for the del Pezzos. As a first step, we construct the metric on \mathbf{X} . Let $h_{a\bar{b}}$ be a Kähler-Einstein metric on dP_n such that $R_{a\bar{b}} = 6h_{a\bar{b}}$. Indeed, we only know of the existence of and not the explicit form¹ of $h_{a\bar{b}}$. We want to consider the case where \mathbf{X} is a cone over dP_n . In this case, the metric on \mathbf{X} can be written [28,29] as

$$ds_{\mathbf{X}}^2 = dr^2 + r^2 \eta^2 + r^2 h_{a\bar{b}} dz^a d\bar{z}^{\bar{b}}, \quad (5.5)$$

where $\eta = (\frac{1}{3}d\psi + \sigma)$. The one-form σ must satisfy $d\sigma = 2\omega$ where ω is the Kähler form on dP_n and $0 \leq \psi < 2\pi$ is the coordinate on the circle bundle over dP_n .

Next, we describe a basis of self-dual and anti-self-dual harmonic forms on dP_n .² We begin with the Kähler form ω . Locally, dP_n looks like \mathbb{C}^2 and $2\omega \sim dz^1 \wedge d\bar{z}^{\bar{1}} + dz^2 \wedge d\bar{z}^{\bar{2}}$. Thus locally, it is easy to see that ω is self-dual under the operation of the Hodge star. Because the Hodge star is a local operator, ω must be self-dual everywhere. Now, recall our dP_n are Einstein. Thus

$$6\omega = iR_{a\bar{b}} dz^a \wedge d\bar{z}^{\bar{b}} = i\partial\bar{\partial} \ln \sqrt{\det h}. \quad (5.6)$$

Clearly $d\omega = (\partial + \bar{\partial})\omega = 0$ whence ω must be closed. It follows that ω is a self-dual harmonic form on dP_n .

There exists a cup product (bilinear form) Q on $H^{1,1}(dP_n)$ defined as

$$Q(\phi, \xi) = \int_{dP_n} \phi \wedge \xi, \quad \phi, \xi \in H^{1,1}(dP_n). \quad (5.7)$$

The Hodge index theorem states that Q has signature $(+, -, \dots, -)$. For dP_n , $h^{2,0} = 0$ while $h^{1,1} = n+1$, there being n other harmonic (1,1) forms on dP_n in addition to ω . We denote these harmonic forms as ϕ_I , $I = 1, \dots, n$. Let us pick a basis for Q such that

$$\phi_I \wedge \omega = 0. \quad (5.8)$$

From the above discussion of ω one sees that

$$0 < \int \omega \wedge \star \omega = \int \omega \wedge \omega, \quad (5.9)$$

where the inequality follows from the definition of the Hodge star and the equality from the fact that ω is self-dual. Hence the ϕ_I span a vector space V where Q has purely negative signature.

Recall that the Hodge star in two complex dimensions squares to one: $\star\star\phi = \phi$. Thus we can diagonalize \star on V such that $\star\phi_I = \pm\phi_I$. However, if $\star\phi_I = \phi_I$, then one would find $\int \phi_I \wedge \phi_I > 0$, in contradiction to the fact that Q has

purely negative signature on V . We conclude that the ϕ_I must all be purely anti-self-dual, $\star\phi_I = -\phi_I$.

With these preliminaries, it is now straightforward to construct G_3 . We let

$$F_3 = \sum_{I=1}^k a^I \eta \wedge \phi_I, \quad H_3 = \sum_{I=1}^k a^I g_s \frac{dr}{r} \wedge \phi_I, \quad (5.10)$$

for expansion coefficients a^I . Hence,

$$G_3 = \sum_{I=1}^k a^I \left(\eta - i \frac{dr}{r} \right) \wedge \phi_I. \quad (5.11)$$

This is a solution because by construction, G_3 is harmonic and is supported on \mathbf{X} so conditions (1) and (4) are met. Moreover, $(dr/r + i\eta)$ is a holomorphic one-form on \mathbf{X} . Therefore, G_3 must have signature (2,1) because ϕ is a (1,1) form. Furthermore, it is easy to check that $\star_{\mathbf{X}} G_3 = iG_3$. Thus, conditions (2) and (3) are also met.

D5-branes. The number of D5-branes in this SUGRA solution is given by the Dirac quantization condition on the RR flux. More precisely, we have an integrality condition on the integral of F_3 over compact three-cycles in the level surface \mathbf{Y} of the cone \mathbf{X} . Given a basis \mathcal{H}^J ($J = 1, \dots, n$) of such cycles, we impose that writing

$$\int_{\mathcal{H}^J} F_3 = 4\pi^2 \alpha' M^J, \quad (5.12)$$

must give integer M^J . From the construction of \mathbf{Y} , it follows that \mathcal{H}^J will be some circle bundle over a curve $D^J \subset dP_n$ while the circumference of the circle is $2\pi/3$. Subsequently, Eq. (5.12) reduces to

$$\sum_I a^I \int_{D^J} \phi_I = 6\pi \alpha' M^J. \quad (5.13)$$

To understand the curve D^J , we take a closer look at the divisors that correspond to elements of $H^{1,1}(dP_n)$. Because dP_n is \mathbb{P}^2 blown up at n points, there will be a divisor H corresponding to the hyperplane in \mathbb{P}^2 and exceptional divisors E_i ($i = 1, \dots, n$) for each of the blow ups. Essentially because two lines intersect at a point, $Q(H, H) = H \cdot H = 1$. From the blow-up construction, we also know that $Q(E_i, E_j) = E_i \cdot E_j = -\delta_{ij}$. Finally, $E_i \cdot H = 0$ because the blow-ups are at general position. We see explicitly that Q has signature $(+, -, -, \dots, -)$. From Poincaré duality, there is a one-to-one map from the differential forms ω and ϕ_I to the divisors H and E_i , which we now explore.

The first chern class of \mathbb{P}^2 is $c_1(\mathbb{P}^2) = 3H$. By the adjunction formula, it follows that $c_1(dP_n) = 3H - \sum_{j=1}^n E_j$. Locally, the first chern class can be expressed in terms of the Ricci tensor,

$$c_1(dP_n) = i \frac{R_{a\bar{b}}}{2\pi} dz^a \wedge d\bar{z}^{\bar{b}}, \quad (5.14)$$

and then from the Einstein condition (5.6), we find that

¹Such a metric is known not to exist for dP_1 and dP_2 . See for example [27].

²We would like to thank Mark Stern and James McKernan for the following argument.

$$\omega = \frac{\pi}{3} c_1(dP_n). \quad (5.15)$$

Thus, by Eq. (5.8), the ϕ_I must be orthogonal to $c_1(dP_n)$. This orthogonality condition has an astonishingly beautiful (and well known) consequence. The orthogonal complement of $3H - \sum_j E_j$ is the weight lattice of the corresponding exceptional Lie group \mathcal{E}_n . In this language the ϕ_I must lie in this weight lattice.

We now return to the following question: what are the curves D^J in the integral (5.13)? The problems we need to worry about in defining the D^J are essentially the same problems we need to worry about in trying to quantize the flux in a far simpler system, that of a collection of point electric charges in three dimensions. In drawing a sphere (or perhaps some shape with more complicated topology) around each charge, we want to make sure that the sphere wraps around the selected charge exactly once and no other charges.

For the dP_n , this condition translates into the requirement that

$$\int_{D^J} \phi_I = \int_{dP_n} \phi_I \wedge c_1(D^J) = \delta_I^J. \quad (5.16)$$

Because $\phi_I \wedge \omega = 0$, only the component of $c_1(D^J)$ orthogonal to $c_1(dP_n)$ need be defined. Let us choose $c_1(D^J) \wedge \omega = 0$. To avoid surrounding charges more than once, we need to make the D^J “as small as possible.” Thus we choose the $c_1(D^J)$ to be the generators of the weight lattice. The condition (5.16) then implies that the ϕ_I generate the root lattice. For example, for dP_3 , we could choose $\phi_1 = E_1 - E_2$, $\phi_2 = E_2 - E_3$, and $\phi_3 = H - E_1 - E_2 - E_3$. Indeed, the bilinear form (5.7) can be written in the basis

$$\int_{dP_n} \phi_I \wedge \phi_J = -A_{IJ}, \quad (5.17)$$

where A_{IJ} is the Cartan matrix for the \mathcal{E}_n root lattice.

Finally, using Eqs. (5.10), (5.13) and (5.16), we can normalize F_3 and H_3 , giving us

$$a^J = 6\pi\alpha' M^J; \quad (5.18)$$

hence the number M^J of D5-branes is fixed in our SUGRA solutions. From a perturbative point of view, we can think of this SUGRA solution as arising from the back reaction of D5-branes wrapped around vanishing curves C_I of \mathbf{X} , which are the Poincaré duals of the ϕ_I . This follows from the definition $dF_3 = \sum a^I d(\eta \wedge \phi_I) = \sum a^I \delta_{C_I}$.

D3-branes. Having discussed some detailed algebraic geometry for the dP_n , we are now ready to quantize the number N of D3-branes as well. The condition reads, using Eq. (5.3),

$$\int_{\mathbf{Y}} F_5 = (4\pi^2 \alpha')^2 N, \quad (5.19)$$

where $F_5 = \mathcal{F} + \star_{10} \mathcal{F}$, and

$$\mathcal{F} = \sum_{I,J} a^I a^J g_s \ln(r/r_0) \eta \wedge \phi_I \wedge \phi_J. \quad (5.20)$$

Therefore one finds, using Eqs. (5.17) and (5.18),

$$N = \frac{3}{2\pi} g_s \ln(r/r_0) \sum_{I,J} M^I A_{IJ} M^J \quad (5.21)$$

for large r . In other words, the number of D3-branes grows logarithmically with the radius.

Warp factor. Now, recalling from [28] that for $\mathbf{Y} = dP_n$,

$$\int_{\mathbf{Y}} \text{vol}(\mathbf{Y}) = \frac{\pi^3}{27} (9-n), \quad (5.22)$$

we can use Eqs. (5.10) and (5.4) to solve for the warp factor. The equation reads

$$\left[\frac{\partial^2}{\partial r^2} + \frac{5}{r} \frac{\partial}{\partial r} \right] Z(r) = \frac{(6\pi\alpha' g_s)^2}{\text{Vol}(\mathbf{Y})} \frac{2\pi}{3r} \sum_{I,J} M^I A_{IJ} M^J. \quad (5.23)$$

This yields

$$Z(r) = \frac{2 \times 3^4}{9-n} \alpha'^2 g_s^2 \left(\frac{\ln(r/r_0)}{r^4} + \frac{1}{4r^4} \right) \sum_{I,J} M^I A_{IJ} M^J. \quad (5.24)$$

In short, we have found the analog of the Klebanov-Tseytlin solution, a solution that is perfectly well behaved at large radius but has a curvature singularity at small radius $Z(r_*) = 0$. We envision that there is some similar warped deformed del Pezzo solution which resolves the singularity, just as the warped deformed conifold of the KS solution resolved the singularity of the KT solution.

C. Gauge couplings

In order to move towards a comparison between SUGRA and gauge theory, let us determine the gauge couplings on probe branes inserted into the geometry we have discussed above. To begin with, let us study D3-branes. Their gauge coupling is simply proportional to the string coupling, g_s , which as we have seen is constant in the self-dual (2,1) solutions. In gauge theory, this is expressed by the fact that the sum of gauge couplings (2.14) is independent of the scale.

We can also probe with D5-branes. Consider a D5-brane wrapped on a curve $C_I \subset dP_n \subset \mathbf{Y}$ at a fixed radial position r in \mathbf{X} . We take C_I to be the Poincaré dual of the harmonic two-form ϕ_I . As is well known (see, e.g., [30]), the gauge coupling on such a brane is related to the integral of the NS 2-form around C_I by

$$x_I = \frac{8\pi^2}{g_I^2} = -\frac{1}{2\pi\alpha' g_s} \int_{C_I} B_2. \quad (5.25)$$

Thus, using the expression for B_2 by integrating H_3 from Eq. (5.10), as well as the value of a^J from Eq. (5.18), we find

$$x_I = -3 \ln r \sum_J \int_{C_I} \phi_J M^J. \quad (5.26)$$

This yields for the beta function

$$\beta_I = \frac{dx_I}{d \ln r} = -3(C_I \cdot C_J) M^J, \quad (5.27)$$

where $C_I \cdot C_J = \int \phi_I \wedge \phi_J$ is the *intersection pairing* of two-cycles in dP_n and the sum on J is implied.

To compare this result with gauge theory, we first need to recall the fact from Sec. II B that a D5 brane wrapped around C_I is associated with a certain combination of fractional branes that we have encoded in the vector $s_I = (s_I^i)$. Thus, the beta function β_I is related to the beta functions of the fractional branes via

$$\beta_I = \sum_i s_I^i \beta_i. \quad (5.28)$$

Inserting the expression for β_i from Eq. (2.10), we obtain the gauge theory expression

$$\beta_I = 3 \sum_i s_I^i s_J^i M^J + \frac{3}{2} \sum_{ij} s_I^i \tilde{R}_{ij} s_J^j M^J, \quad (5.29)$$

where \tilde{R} is given in Eq. (2.11). Let us now use the vanishing of the beta function for the conformal theory [corresponding to putting $d^i = r^i$ in Eq. (2.8) and using Eq. (2.10)] to rewrite the first term as

$$\sum_i s_I^i s_J^i = -\frac{1}{2} \sum_{ij} s_I^i s_J^j \tilde{R}_{ij} \frac{r^j}{r^i}. \quad (5.30)$$

Using the definition of \tilde{R}_{ij} in Eq. (2.11), we find the gauge theory result

$$\begin{aligned} \beta_I &= \frac{3}{2} \sum_{ij} \tilde{R}_{ij} \left(s_I^i s_J^j - s_I^j s_J^i \frac{r^j}{r^i} \right) M^J \\ &= \frac{3}{2} \sum_{ij} f_{ij}(R_{ij} - 1) \left(s_I^i s_J^j + s_I^j s_J^i \frac{r^j}{r^i} \right. \\ &\quad \left. - s_I^j s_J^i \frac{r^j}{r^i} \right) M^J. \end{aligned} \quad (5.31)$$

To finish up and relate this long-winded expression to the intersection pairing in Eq. (5.27), we need to rely on certain results concerning baryonic $U(1)$ charges in quiver gauge theories related to del Pezzos [2,7,12,31]. First of all, these baryonic $U(1)$ charges are in one-to-one correspondence with possible nonconformal deformations. In formulas, one can write all baryonic $U(1)$ charges Q_I as a sum

$$Q_I = \sum_i q_I^i Q_i, \quad (5.32)$$

where Q_i is a charge associated with the nodes of the quiver and is equal to $+1$ for incoming arrows and -1 for outgoing arrows. In other words,

$$Q_I(X_{ij}) = q_I^j - q_I^i. \quad (5.33)$$

For purposes of anomaly cancellation, these charges are related to the null vectors s_I^i of $\mathcal{I} = S - S'$ via [7,12]

$$q_I^i r^i = s_I^i. \quad (5.34)$$

It was then shown in [12] that the baryonic $U(1)$ charges Q_I are also in one-to-one correspondence with curves C_I in the del Pezzo orthogonal to the Kähler class. Moreover, it was shown in [12] that one could identify the intersection product of the curves C_I as the cubic anomaly associated with the baryonic charges Q_I ,

$$C_I \cdot C_J = \frac{1}{2} \text{tr} R Q_I Q_J. \quad (5.35)$$

Now let us relate this cubic anomaly to the beta functions

$$\begin{aligned} (\text{tr} R Q_I Q_J) M^J &= M^J \sum_{i,j} f_{ij}(R_{ij} - 1) Q_I(X_{ij}) Q_J(X_{ij}) r^i r^j \\ &= M^J \sum_{i,j} f_{ij}(R_{ij} - 1) (q_I^j - q_I^i) (q_J^j - q_J^i) r^i r^j \\ &= -M^J \sum_{i,j} f_{ij}(R_{ij} - 1) \left(s_I^i s_J^j + s_I^j s_J^i \frac{r^j}{r^i} \right. \\ &\quad \left. - s_I^j s_J^i \frac{r^j}{r^i} - s_I^i s_J^j \frac{r^j}{r^i} \right) = -\frac{2}{3} \beta_I. \end{aligned}$$

This expression, upon substituting into the SuGRA result (5.27) gives the gauge theory result for the beta function in Eq. (5.31), whereby giving us the link we needed.

D. Discussion

On the one hand it is impressive that we can write down such a complicated supergravity solution that encodes interesting field theoretic behavior without knowing the precise metric on the del Pezzos. On the other, it is a little disappointing that we have found no smoking gun for the existence of duality walls from the supergravity perspective.

Let us consider the implications of this KT-like solution for del Pezzos. Such a solution indicates that the dual del Pezzo field theory should behave like the KS field theory. In other words, one expects a sequence of Seiberg dualities where as we move into the UV, the number of D3-branes gradually increases, the number of D5-branes remains fixed, and no duality wall is reached. We have seen such behavior for some of the phases of the del Pezzos. For example, the model A or model B flow of [5] and the dP_1 flow considered here exhibit such behavior. We expect that such flows can probably be constructed for all del Pezzos.

Our supergravity solutions severely constrain possible $\mathcal{O}(M/N)$ corrections to the R-charges for KS type flows. In particular, both on the field theory side and on the supergravity side, we saw that the sum of the beta functions (2.14) must vanish. Additionally, we calculated the $n \beta_i$ for dP_n both in field theory and in supergravity and saw that the two expressions agreed. In total, we have $n+1$ constraints on $n+3$ beta functions. Thus, any corrections to the beta functions for KS flows must lie in the remaining two dimensional vector space. (Note that for the original KT solution for the conifold, the two constraints are enough to eliminate any possible corrections to the two beta functions.)

We have also seen behavior vastly different from KS type cascades. For example, for the F_0 surface, we saw duality walls. Note also in this flow that the number of D3-branes does not increase but is pinned by nodes three and four. Presumably there is some other supergravity solution which describes this flow. One way of constructing a more general type of supergravity solution would be to try to construct F_3 with a dependence on dr or to start with a nonconical metric on \mathbf{X} .

ACKNOWLEDGMENTS

We would like to thank Jerome Gauntlett, Ami Hanany, Aki Hashimoto, James McKernan, Rob Myers, Joe Polchinski, Mark Stern and Cumrun Vafa for useful discussions. This research is funded in part by the CTP and the LNS of MIT and by the department of Physics at UPenn. The research of S.F. was supported in part by U.S. DOE Grant No. DE-FC02-94ER40818. The research of Y.-H.H. was supported in part by U.S. DOE Grant No. DE-FG02-95ER40893 as well as an NSF Focused Research Grant No. DMS0139799 for “The Geometry of Superstrings.” The research of C.H. and J.W. was supported in part by the NSF under Grant No. PHY99-07949.

APPENDIX: SEIBERG DUALITY AND THE BETA FUNCTION

We show how to demonstrate that after Seiberg duality on node i of a four-node, well split quiver, the value of β_i changes sign. The proof makes extensive use of results from [11].

Any well split, four-node quiver can be represented by the matrix,

$$S = \begin{pmatrix} 1 & a & b & c \\ 0 & 1 & d & e \\ 0 & 0 & 1 & f \\ 0 & 0 & 0 & 1 \end{pmatrix} \quad (\text{A1})$$

where all the entries are integers, $b \geq 0$, $c \geq 0$, and a, d, e , and f are non-positive [11]. Note that one may have to cyclically permute the ordering of the nodes to satisfy these sign requirements. In [11] such a quiver was called A_i . The cyclic permutations were labeled A_{ii} , A_{iii} , and A_{iv} . The conditions that S be rank two and that $\text{Tr} S S^{-T} = 4$ put the following two constraints on the matrix entries:

$$cd - be + af = 0 \quad (\text{A2})$$

and

$$a^2 + b^2 + c^2 + d^2 + e^2 + f^2 - abd - ace - bcf - def + acdf = 0. \quad (\text{A3})$$

In order to compute the beta functions, we also need expressions for the ranks of the gauge groups at the conformal point. Again from [11], we find that

$$\begin{aligned} 8r_1^2 &= d^2 + e^2 + f^2 - def, & 8r_2^2 &= b^2 + c^2 + f^2 - bcf, \\ 8r_3^2 &= a^2 + c^2 + e^2 - ace, & 8r_4^2 &= a^2 + b^2 + d^2 - abd, \\ 8r_1 r_2 &= cdf - bd - ce, & 8r_1 r_3 &= ad - cf, \\ 8r_1 r_4 &= ae + bf - adf, \\ 8r_2 r_3 &= acf - ab - ef, & 8r_2 r_4 &= -ac + fd, \\ 8r_3 r_4 &= acd - de - bc. \end{aligned} \quad (\text{A4})$$

Note that these values of the r_i are independent of the signs of the entries of S .

Finally, we need to know how many D5-branes are present. $S - S^T$ has only a two dimensional kernel. We know that r is one element of the kernel. From Eq. (A2), we can read off another, linearly independent element $s = (0, f, -e, d)$. The vectors s and r span the kernel, and we will assume we have one D5-brane, $M=1$, of the type s .

We now have enough to compute the beta functions using Eqs. (2.9) and (2.10). The expressions are messy, and we will not reproduce them here.

To verify that the β_i flips sign after Seiberg duality on node i , we have to see what happens to our quiver after duality on nodes 1, 2, 3, and 4.

Node 1. After Seiberg duality on node 1, the resulting quiver can be described by the matrix

$$S_1 = \begin{pmatrix} 1 & a & d-ab & e-ac \\ 0 & 1 & -b & -c \\ 0 & 0 & 1 & f \\ 0 & 0 & 0 & 1 \end{pmatrix} \quad (\text{A5})$$

and the vector s is transformed into $s' = (f, -af, -e, d)$. The r_i are still given by Eq. (A4) but with the appropriate substitutions indicated by S_1 .

Note that Seiberg duality changes the ordering of the nodes. After duality, node 1 becomes node 2. Thus, we checked using a computer algebra package and the relations (A2) and (A3) that $\beta_1 + \beta_2' = 0$.

Node 2. After Seiberg duality on node 2, the resulting quiver can be described by the matrix

$$S_2 = \begin{pmatrix} 1 & a & -d & -e \\ 0 & 1 & b-ad & c-ea \\ 0 & 0 & 1 & f \\ 0 & 0 & 0 & 1 \end{pmatrix} \quad (\text{A6})$$

and the vector s is transformed into $s' = (-f, 0, -e, d)$.

After duality, node 2 becomes node 1. Thus, we checked that $\beta_2 + \beta'_1 = 0$.

Node 3. After Seiberg duality on node 3, the resulting quiver can be described by the matrix

$$S_3 = \begin{pmatrix} 1 & -b & a-bd & c \\ 0 & 1 & d & -f \\ 0 & 0 & 1 & e-fd \\ 0 & 0 & 0 & 1 \end{pmatrix} \quad (\text{A7})$$

and the vector s is transformed into $s' = (0, e-df, f, d)$.

After duality, node 3 becomes node 2. Thus, we checked that $\beta_3 + \beta'_2 = 0$.

Node 4. After Seiberg duality on node 4, the resulting quiver can be described by the matrix

$$S_4 = \begin{pmatrix} 1 & e & f & c \\ 0 & 1 & d & -a+ce \\ 0 & 0 & 1 & -b+cf \\ 0 & 0 & 0 & 1 \end{pmatrix} \quad (\text{A8})$$

and the vector s is transformed into $s' = (-d, f, -e, 0)$.

After duality, node 4 becomes node 1. Thus, we checked that $\beta_4 + \beta'_1 = 0$.

-
- [1] A.E. Lawrence, N. Nekrasov, and C. Vafa, Nucl. Phys. **B533**, 199 (1998); S. Kachru and E. Silverstein, Phys. Rev. Lett. **80**, 4855 (1998); A. Kehagias, Phys. Lett. B **435**, 337 (1998); B.S. Acharya, J.M. Figueroa-O'Farrill, C.M. Hull, and B. Spence, Adv. Theor. Math. Phys. **2**, 1249 (1999); I.R. Klebanov and E. Witten, Nucl. Phys. **B536**, 199 (1998).
- [2] D.R. Morrison and M.R. Plesser, Adv. Theor. Math. Phys. **3**, 1 (1999).
- [3] I.R. Klebanov and M. Strassler, J. High Energy Phys. **08**, 052 (2000).
- [4] A. Hanany and J. Walcher, J. High Energy Phys. **06**, 055 (2003).
- [5] S. Franco, A. Hanany, Y.H. He, and P. Kazakopoulos, "Duality walls, duality trees and fractional branes," hep-th/0306092; S. Franco, A. Hanany, and Y.H. He, "A trio of dualities: Walls, trees and cascades," hep-th/0312222.
- [6] K. Intriligator and B. Wecht, Nucl. Phys. **B667**, 183 (2003).
- [7] K. Intriligator and B. Wecht, "Baryon charges in 4D superconformal field theories and their AdS duals," hep-th/0305046.
- [8] B. Fiol, J. High Energy Phys. **07**, 058 (2002).
- [9] M. J. Strassler, "Duality in Supersymmetric Field Theory and an Application to Real Particle Physics," talk given at International Workshop on Perspectives of Strong Coupling Gauge Theories (SCGT 96), Nagoya, Japan. Available at <http://www.eken.phys.nagoya-u.ac.jp/Scgt/proc/>
- [10] F. Cachazo, B. Fiol, K.A. Intriligator, S. Katz, and C. Vafa, Nucl. Phys. **B628**, 3 (2002).
- [11] C.P. Herzog, "Exceptional Collections and del Pezzo Gauge Theories," hep-th/0310262.
- [12] C.P. Herzog and J. Walcher, J. High Energy Phys. **09**, 060 (2003).
- [13] A. Morozov and A.J. Niemi, Nucl. Phys. **B666**, 311 (2003); A. Leclair, J.M. Roman, and G. Sierra, *ibid.* **B675**, 584 (2003).
- [14] M. Graña and J. Polchinski, Phys. Rev. D **63**, 026001 (2001).
- [15] I.R. Klebanov and A.A. Tseytlin, Nucl. Phys. **B578**, 123 (2000).
- [16] V.A. Novikov, M.A. Shifman, A.I. Vainshtein, and V.I. Zakharov, Nucl. Phys. **B229**, 381 (1983).
- [17] C. Beasley, B.R. Greene, C.I. Lazaroiu, and M.R. Plesser, Nucl. Phys. **B566**, 599 (2000).
- [18] B. Feng, A. Hanany, and Y.H. He, Nucl. Phys. **B595**, 165 (2001); J. High Energy Phys. **08**, 040 (2001); B. Feng, S. Franco, A. Hanany, and Y.H. He, *ibid.* **08**, 058 (2003).
- [19] B. Feng, A. Hanany, Y.H. He, and A.M. Uranga, J. High Energy Phys. **12**, 035 (2001); B. Feng, S. Franco, A. Hanany, and Y.H. He, *ibid.* **12**, 076 (2002).
- [20] S. Franco and A. Hanany, J. High Energy Phys. **04**, 043 (2003); Fortsch. Phys. **51**, 738 (2003).
- [21] B. Feng, A. Hanany, Y.H. He, and A. Iqbal, J. High Energy Phys. **02**, 056 (2003).
- [22] D. Anselmi, J. Erlich, D.Z. Freedman, and A.A. Johansen, Phys. Rev. D **57**, 7570 (1998); D. Anselmi, D.Z. Freedman, M.T. Grisaru, and A.A. Johansen, Nucl. Phys. **B526**, 543 (1998).
- [23] K. Becker and M. Becker, Nucl. Phys. **B477**, 155 (1996).
- [24] S. Gukov, C. Vafa, and E. Witten, Nucl. Phys. **B584**, 69 (2000); **B608**, 477(E) (2001).
- [25] K. Dasgupta, G. Rajesh, and S. Sethi, J. High Energy Phys. **08**, 023 (1999).
- [26] S.S. Gubser, "Supersymmetry and F-theory realization of the deformed conifold with three-form flux," hep-th/0010010.
- [27] G. Tian, Invent. Math. **137**, 1 (1997).
- [28] A. Bergman and C.P. Herzog, J. High Energy Phys. **01**, 030 (2002).
- [29] D. Berenstein, C.P. Herzog, and I.R. Klebanov, J. High Energy Phys. **06**, 047 (2002).
- [30] C.P. Herzog, I.R. Klebanov, and P. Ouyang, "Remarks on the warped deformed conifold," hep-th/0108101.
- [31] C.P. Herzog and J. McKernan, J. High Energy Phys. **08**, 054 (2003).